

## Self-Supported Cobalt Nickel Nitride Nanowires Electrode for Overall Electrochemical Water Splitting

Lei Han, Kun Feng, and Zhongwei Chen\*<sup>[a]</sup>

The design and synthesis of electrocatalysts possessing both hydrogen and oxygen evolution activity is of critical importance to simplify the water splitting system. In this work, we reported the preparation of porous Ni–Co nitride nanowires (NiCoN NWs) supported on carbon cloth, and used as bifunctional electrocatalysts to achieve overall water splitting. Benefiting from the 1D porous nanowire structure, the close contact between catalysts and support, and the increased conductivity, the resultant NiCoN NWs exhibited high activities in both the hydrogen and oxygen evolution reactions (HER and OER) with low overpotential at a current density of  $10 \text{ mA cm}^{-2}$  ( $\approx 145 \text{ mV}$  for HER and  $360 \text{ mV}$  for OER), low Tafel slope ( $105.2 \text{ mV dec}^{-1}$  for HER and  $46.9 \text{ mV dec}^{-1}$  for OER), and good electrochemical stability. Good stability was also obtained upon using the material as HER and OER catalysts in a two-electrode system to split water.

Increasing energy demand and environmental concerns have triggered scientific and industrial interests in exploiting renewable and clean energy sources.<sup>[1–6]</sup> Among them, hydrogen energy is regarded as the most promising renewable energy carrier alternative to traditional fossil fuels due to the high gravimetric energy density and low environmental pollution without carbon emissions.<sup>[7]</sup> Recently, considerable efforts have been made to develop various methods for efficient hydrogen production. Particularly, electrochemical water splitting provides an efficient and environmentally friendly strategy, which is composed of two reactions: oxygen and hydrogen evolution.<sup>[3,8]</sup> To achieve water splitting efficiently, it is of importance to develop a highly efficient and stable electrocatalyst to expedite these reactions. Currently, the state-of-the-art reported electrocatalysts for water splitting mainly focus on noble metal materials, such as Pt for the hydrogen evolution reaction (HER) and  $\text{IrO}_2$  for the oxygen evolution reaction (OER).<sup>[7,9]</sup> However, the high cost and the rarity of the materials make their practical applications unattractive. Therefore, it is still urgently needed, but remains a challenge, to explore novel non-noble electrocatalysts with low-cost and high catalytic activity.

In recent decades, transition-metal-based materials have been extensively studied due to their potential for energy-re-

lated applications such as water splitting.<sup>[10–13]</sup> Up to now, various transition-metal-based oxides/hydroxides, phosphides, sulfides, selenides, and carbides, have been reported as electrocatalysts to exhibit appreciable electrocatalytic activity toward HER or OER.<sup>[7,12–16]</sup> Although some progress has been achieved, there is still significant room for improvement. First of all, the poor electron conductivity of these electrocatalysts largely restricts the electron transport between the catalyst surface and the support electrode, thus resulting in high overpotential and low energy conversion efficiency.<sup>[17–19]</sup> Secondly, most of them generally have a single function, that is, they can only efficiently catalyze the HER or OER, which makes the water splitting system complicated and increases the hydrogen production cost. These limitations have stimulated extensive efforts to explore novel materials to boost OER and HER. Recently, transition-metal-based nitrides (TMNs) have received increasing attention owing to their unique physiochemical properties such as high electrical conductivity and good chemical stability.<sup>[8,11,13,20]</sup> Theoretical calculations demonstrated that, compared to metal oxides, the increased electrical conductivity was mainly due to the introduction of nitrogen, which strongly modifies the electronic structure of the metal host.<sup>[21,22]</sup> These advantages of TMNs endow them with excellent catalytic activity for energy related applications.<sup>[23–25]</sup> For example, metallic  $\text{Ni}_3\text{N}$  nanosheets and  $\text{Co}_4\text{N}$  porous nanowires have been prepared as OER electrocatalysts and have exhibited good electrocatalytic performance.<sup>[5,19,21,26]</sup> Other nitrides such as Co–Mo and Ni–Mo nitrides have also been reported to possess high HER electrochemical activity.<sup>[1,22]</sup> However, little work has been performed to explore transition-metal nitrides as bifunctional electrocatalysts to achieve overall water splitting. Herein, porous Ni–Co nitride (NiCoN) nanowires supported on carbon cloth have been successfully prepared by annealing Ni–Co precursors (NiCo layered double hydroxides, NiCo-LDHs) under ammonia and exhibited good HER and OER performances. It is well accepted that the electrochemical performances of the electrocatalysts are strongly dependent on their composites and morphologies. Compared to monometallic nitrides, bimetallic nitrides possess more active sites and enhanced electronic conductivity, thus achieving easily the high electrochemical performances. In addition, the high specific surface area and fast electron transport rate of the obtained porous nanowires structure are also beneficial for improving the electrocatalytic performance.

The preparation procedure of porous Co–Ni nitride nanowires is depicted in Figure 1. The NiCo-LDHs were first prepared by using a hydrothermal method, and the sample was then treated under ammonia at high temperature for 1 h to obtain NiCoN (noted as NiCoN-1H). The scanning electron

[a] Dr. L. Han, K. Feng, Prof. Z. W. Chen  
Department of Chemical Engineering  
University of Waterloo  
200 University Avenue West  
Waterloo, Ontario, N2L3G1 (Canada)  
E-mail: zhwenchen@uwaterloo.ca

Supporting Information for this article can be found under:  
<https://doi.org/10.1002/ente.201700108>.

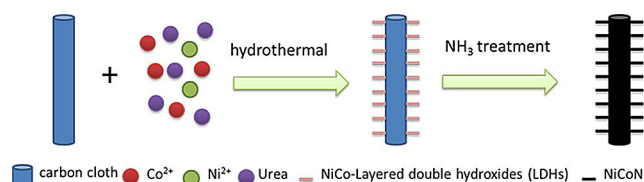


**Figure 1.** Schematic illustration of the synthesis route for cobalt nickel nitride nanowires supported on carbon cloth.

microscopy (SEM) images (Figure S1, Supporting Information) clearly demonstrated that smooth NiCo-LDH nanowires were uniformly coated on the surface of the carbon cloth. After ammonia treatment, the as-prepared NiCoN still retained one-dimensional nanowire structures but their surfaces became rougher compared to the as-prepared NiCo-LDHs (Figure 2). We also observed that these nanowires in-

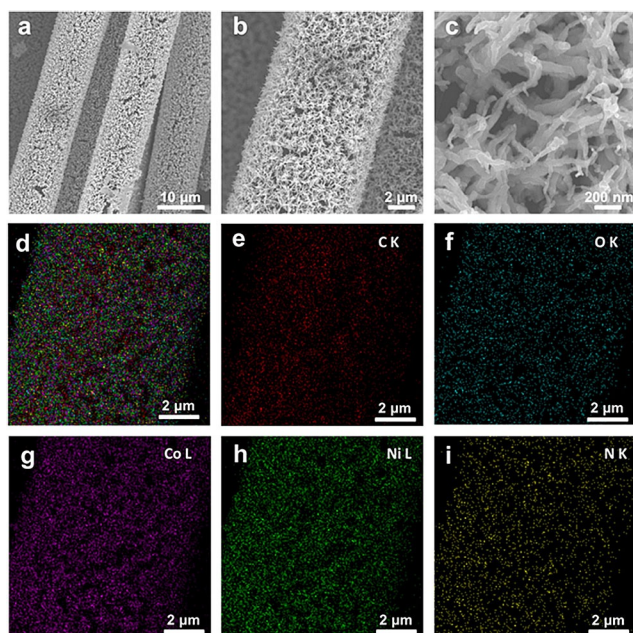


**Figure 2.** SEM images (a–c) and the corresponding element mapping (d–i) of the as-prepared NiCoN-1H/CC obtained by annealing under NH<sub>3</sub> at 500 °C for 1 h.

terconnected together to construct a network-like structure, which provided large surface area, fast mass transfer, and good electrical conductivity. For comparison, we also prepared NiCoN by annealing the NiCo-LDHs annealed under ammonia at 500 °C for 5 h (noted as NiCoN-5H). As shown in Figure S2 (Supporting Information), the as-prepared NiCoN-5H exhibits similar morphology to NiCoN-1H. During the nitriding process, the morphology transformation may be due to the etching effect of ammonia by reacting with Co and/or Ni at high temperature. The chemical composite of the as-prepared NiCoN was examined by energy-dispersive X-ray spectroscopy (EDX), and the results are shown in Figure S3 and Table S1 (Supporting Information). As shown, the atom ratio of Ni/Co/N was approximately

1:2:2. The corresponding elemental mapping analysis (Figure 2d–i) also verifies the uniform spatial distribution of Co, Ni, and N throughout the porous NiCoN nanowires, which is in agreement with the results of EDX. The crystal structures of the as-prepared NiCo-LDHs and NiCoN were investigated by X-ray diffraction (XRD) (Figure S4a, Supporting Information). As observed, the peak at 43.2° for NiCo-LDHs is shifted to 44.6° for NiCoN, which further confirms the successful preparation of NiCoN.

X-ray photoelectron spectroscopy (XPS) was conducted to investigate the surface chemical composite and states of the products. For NiCo-LDHs, the Ni 2p spectrum (Figure S4b, Supporting Information) shows that the peaks at 854 eV (Ni 2p<sub>3/2</sub>), 856 eV (Ni 2p<sub>3/2</sub>), and 872.6 eV (Ni 2p<sub>1/2</sub>) are ascribed to the +2 oxidation state of Ni, whereas the other two peaks at 861.5 and 879.5 eV are attributed to the Ni satellite peaks in NiO.<sup>[18,27]</sup> For the Co spectra (Figure S4c, Supporting Information), the peaks at 780.3 and 796.2 eV can be assigned to the +2 oxidation state of Co, and the peak at 786.2 eV is attributed to Co–OH bonds.<sup>[17]</sup> After annealing the NiCo-LDHs under ammonia, it was observed that the Ni 2p peaks of NiCoN-1H clearly shift into higher binding energy than those of NiCo-LDHs (Figure S4b, Supporting Information). The peaks at 859.5 and 876.3 eV in the Ni 2p spectra of NiCoN-1H indicate the presence of Ni<sup>2+</sup>, and the peaks at 864.3 and 882.2 eV correspond to the metallic state of Ni in NiCoN-1H, suggesting that Ni<sup>2+</sup> ions were partially reduced by the thermal treatment of ammonia.<sup>[27,28]</sup> The peak located at 783.9 eV was also observed in the Co 2p spectrum, which can be attributed to the Co<sup>3+</sup>–O/N bonds.<sup>[17]</sup> Additionally, there is a peak at 400.7 eV in the N 1s spectrum region, which is ascribed to the nitrogen in the metal nitrides (Figure S4d, Supporting Information).<sup>[18]</sup>

The electrocatalytic HER activity of the resultant porous NiCoN nanowires was firstly investigated by using a standard three-electrode system under alkaline conditions. For comparison, a carbon cloth was also treated under the same conditions (noted as CC-NH<sub>3</sub>). Figure 3a presents the HER polarization curves of the resultant CC-NH<sub>3</sub>, NiCo-LDHs, NiCoN-5H, and NiCoN-1H in 1.0 M NaOH. As shown, the resultant CC-NH<sub>3</sub> and NiCo-LDHs both exhibited poor electrocatalytic activity toward the HER. In contrast, the resultant NiCoN-1H exhibits the highest electrocatalytic activity, and a low overpotential of 145 mV is only required to reach a current density of 10 mA cm<sup>-2</sup>, which is comparable to that of the reported other transition-metal nitrides.<sup>[1, 8, 9, 20, 21, 28, 29]</sup> However, when the annealing time under ammonia is prolonged to 5 h, the resultant NiCoN-5H shows decreased electrocatalytic activity, which requires a higher overpotential (168 mV) to achieve the same current density. The decreased catalytic activity may be due to the etching effect of ammonia itself, which results in the decreased activity of NiCoN supported on carbon cloth. Then we investigated the Tafel plots of the resultant electrodes (Figure 3b). We observed that the resultant NiCoN-1H possesses a lower Tafel slope (105.2 mV dec<sup>-1</sup>) than the resultant NiCoN-5H, indicating the more favorable HER kinetics in alkaline solution. As we

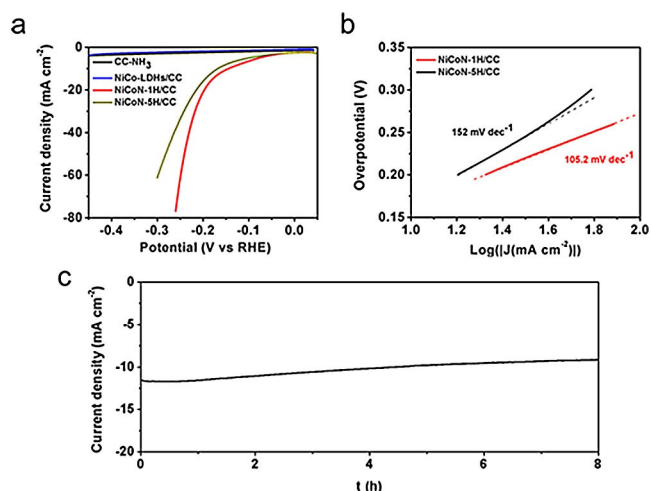


**Figure 3.** Electrochemical HER activity evaluation of the resultant modified electrodes in 1.0 M NaOH: (a) polarization curves ( $iR$ -corrected) at a scan rate of  $5 \text{ mV s}^{-1}$ , (b) Tafel slopes, and (c) time-dependent current density curves under  $\eta = 174 \text{ mV}$ .

know, the stability of catalysts is also important for their practical applications. The stability was also evaluated by measuring the current–time curves at an overpotential of 174 mV. It is shown in Figure 3c that there is no obvious decrease, suggesting the good stability. We further investigated the OER activity of the resultant electrodes. Figure 4a pres-

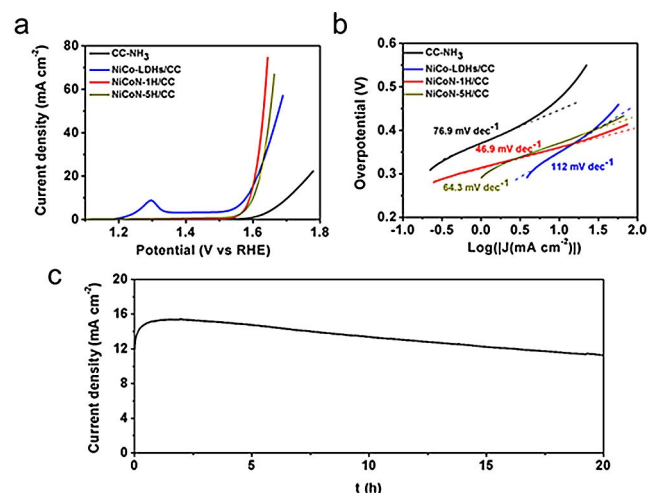


**Figure 4.** Electrochemical OER activity evaluation of the resultant modified electrodes in 1.0 M NaOH: (a) polarization curves ( $iR$ -corrected) at a scan rate of  $5 \text{ mV s}^{-1}$ , (b) Tafel slopes, and (c) time-dependent current density curves under  $\eta = 380 \text{ mV}$ .

ents the OER polarization curves of the resultant CC-NH<sub>3</sub>, NiCo-LDHs, NiCoN-5H, and NiCoN-1H samples in 1.0 M NaOH. It is noted that the resultant CC-NH<sub>3</sub> exhibited poor electrocatalytic activity toward OER. Although the resultant NiCo-LDHs shows a low onset potential, the resultant NiCoN needs lower overpotential at high current density regardless of the ammonia heat treatment time. Moreover, only an overpotential of 360 mV is required to achieve a cur-

rent density of  $10 \text{ mA cm}^{-2}$ , which is comparable to that of NiCo-LDHs (350 mV). Then the Tafel plots of the resultant different electrodes in 1 M NaOH were also investigated, and the results are shown in Figure 4b. Among them, the resultant NiCoN-1H presents the smallest Tafel slope ( $46.9 \text{ mV dec}^{-1}$ ), indicating the more favorable OER kinetics in alkaline solution. Moreover, the resultant NiCoN-1H also exhibits excellent stability (Figure 4c).

To explore the factors influencing the electrocatalytic activity, we measured the electrochemical impedance spectroscopy (EIS) and electrochemically active surface area (ECSA). The EIS results (Figure S5, Supporting Information) reveal that NiCoN-1H possesses a smaller charge-transfer resistance than the NiCoN-5H and NiCo-LDHs, and this is beneficial for improving the electrocatalytic performance. For additional information, the ECSA is usually estimated by measuring the electrochemical double-layer capacitance ( $C_{dl}$ ) because the  $C_{dl}$  of catalysts is generally proportional to ECSA.<sup>[30]</sup> It is observed from Figure S6–8 (Supporting Information) that the NiCo-LDHs exhibit the largest ECSA whereas the NiCoN-1H has the smallest ECSA. Therefore, the enhanced electrocatalytic activity of the resultant NiCoN-1H is mainly attributed to the increased conductivity owing to the introduction of nitrogen. Additionally, the 1D porous nanowires structure and 3D framework of the carbon cloth as an excellent conductive substrate facilitate the electron transport and mass transfer. Moreover, the close contact between the NiCoN nanowires and carbon cloth are also ascribed to the improved long-term stability. Finally we used NiCoN-1H as HER and OER catalysts in a two-electrode electrolyzer to achieve overall water splitting. As depicted in Figure 5, the current density reaches  $13 \text{ mA cm}^{-2}$  at an overpotential of 570 mV, and can be maintained at over 79% of this value after 8 h.

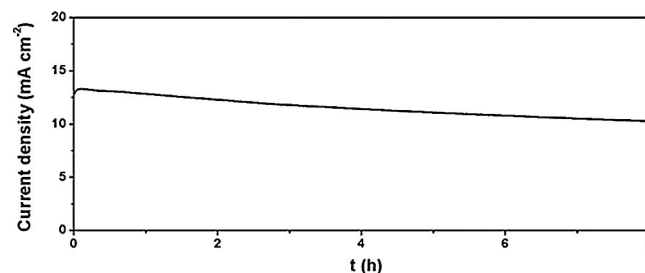


**Figure 5.** Time-dependent current density curves of overall water splitting under  $\eta = 570 \text{ mV}$  in 1.0 M NaOH.

In summary, we have successfully prepared porous NiCoN nanowires supported on carbon cloth by using hydrothermal synthesis followed by heat treatment under ammonia. The electrochemical results demonstrated that the resultant porous NiCoN nanowires exhibited high HER and OER electrocatalytic activity in alkaline solution with a small overpotential at a current density of  $10 \text{ mA cm}^{-2}$  ( $\approx 145 \text{ mV}$  for HER and  $360 \text{ mV}$  for OER), low Tafel slope ( $105.2 \text{ mV dec}^{-1}$  for HER and  $46.9 \text{ mV dec}^{-1}$  for OER), and good electro-

chemical stability. The enhanced electrocatalytic activity is attributed to the following factors: the increased conductivity owing to the introduction of nitrogen, the 1D porous nanowires structure, and the close contact between catalysts (NiCoN) and support (carbon cloth). Good stability was also obtained upon assembly of the porous NiCoN nanowires as HER and OER catalysts to achieve overall water splitting, which suggests its attractive potential as a bifunctional electrocatalyst for this application.

## Acknowledgements

The authors acknowledge the financial support from the Natural Sciences and Engineering Research Council of Canada (NSERC), the University of Waterloo, and the Waterloo Institute for Nanotechnology.

## Conflict of interest

The authors declare no conflict of interest.

**Keywords:** carbon cloth • electrochemistry • cobalt nickel nitride • hydrogen evolution • water splitting

- [1] B. Cao, G. M. Veith, J. C. Neuefeind, R. R. Adzic, P. G. Khalifah, *J. Am. Chem. Soc.* **2013**, *135*, 19186–19192.
- [2] F. Meng, H. Zhong, D. Bao, J. Yan, X. Zhang, *J. Am. Chem. Soc.* **2016**, *138*, 10226–10231.
- [3] Y. Zhang, B. Ouyang, J. Xu, G. Jia, S. Chen, R. S. Rawat, H. J. Fan, *Angew. Chem. Int. Ed.* **2016**, *55*, 8670–8674; *Angew. Chem.* **2016**, *128*, 8812–8816.
- [4] W. F. Chen, K. Sasaki, C. Ma, A. I. Frenkel, N. Marinkovic, J. T. Muckerman, Y. Zhu, R. R. Adzic, *Angew. Chem. Int. Ed.* **2012**, *51*, 6131–6135; *Angew. Chem.* **2012**, *124*, 6235–6239.
- [5] P. Chen, K. Xu, Z. Fang, Y. Tong, J. Wu, X. Lu, X. Peng, H. Ding, C. Wu, Y. Xie, *Angew. Chem. Int. Ed.* **2015**, *54*, 14710–14714; *Angew. Chem.* **2015**, *127*, 14923–14927.
- [6] L. Han, S. Dong, E. Wang, *Adv. Mater.* **2016**, *28*, 9266–9291.
- [7] L. Han, M. Xu, Y. Han, Y. Yu, S. Dong, *ChemSusChem* **2016**, *9*, 2784–2787.
- [8] S. Li, Y. Wang, S. Peng, L. Zhang, A. M. Al-Enizi, H. Zhang, X. Sun, G. Zheng, *Adv. Energy Mater.* **2016**, *6*, 1501661.
- [9] X. Jia, Y. Zhao, G. Chen, L. Shang, R. Shi, X. Kang, G. I. N. Waterhouse, L.-Z. Wu, C.-H. Tung, T. Zhang, *Adv. Energy Mater.* **2016**, *6*, 1502585.
- [10] D. Zhao, Z. Cui, S. Wang, J. Qin, M. Cao, *J. Mater. Chem. A* **2016**, *4*, 7914–7923.
- [11] H. Hu, B. Y. Guan, X. W. Lou, *Chemistry* **2016**, *1*, 102–113.
- [12] G. Li, X. Wang, J. Fu, J. Li, M. G. Park, Y. Zhang, G. Lui, Z. Chen, *Angew. Chem. Int. Ed.* **2016**, *55*, 4977–4982; *Angew. Chem.* **2016**, *128*, 5061–5066.
- [13] J. Fu, F. M. Hassan, J. Li, D. U. Lee, A. R. Ghannoum, G. Lui, M. A. Hoque, Z. Chen, *Adv. Mater.* **2016**, *28*, 6421–6428.
- [14] R. Wu, Y. Xue, B. Liu, K. Zhou, J. Wei, S. H. Chan, *J. Power Sources* **2016**, *330*, 132–139.
- [15] X. Li, Q. Jiang, S. Dou, L. Deng, J. Huo, S. Wang, *J. Mater. Chem. A* **2016**, *4*, 15836–15840.
- [16] H. Hu, B. Guan, B. Xia, X. W. Lou, *J. Am. Chem. Soc.* **2015**, *137*, 5590–5595.
- [17] Y. Wang, D. Liu, Z. Liu, C. Xie, J. Huo, S. Wang, *Chem. Commun.* **2016**, *52*, 12614–12617.
- [18] Y. Wang, C. Xie, D. Liu, X. Huang, J. Huo, S. Wang, *ACS Appl. Mater. Interfaces* **2016**, *8*, 18652–18657.
- [19] D. Gao, J. Zhang, T. Wang, W. Xiao, K. Tao, D. Xue, J. Ding, *J. Mater. Chem. A* **2016**, *4*, 17363–17369.
- [20] Y. Han, X. Yue, Y. Jin, X. Huang, P. K. Shen, *J. Mater. Chem. A* **2016**, *4*, 3673–3677.
- [21] M. Shalom, D. Ressnig, X. Yang, G. Clavel, T. P. Fellinger, M. Antonietti, *J. Mater. Chem. A* **2015**, *3*, 8171–8177.
- [22] Y. Zhang, B. Ouyang, J. Xu, S. Chen, R. S. Rawat, H. J. Fan, *Adv. Energy Mater.* **2016**, *6*, 1600221.
- [23] M.-S. Balogun, W. Qiu, H. Yang, W. Fan, Y. Huang, P. Fang, G. Li, H. Ji, Y. Tong, *Energy Environ. Sci.* **2016**, *9*, 3411–3416.
- [24] M.-S. Balogun, W. Qiu, F. Lyu, Y. Luo, H. Meng, J. Li, W. Mai, L. Mai, Y. Tong, *Nano Energy* **2016**, *26*, 446–455.
- [25] M.-S. Balogun, Y. Zeng, W. Qiu, Y. Luo, A. Onasanya, T. K. Olaniyi, Y. Tong, *J. Mater. Chem. A* **2016**, *4*, 9844–9849.
- [26] P. Chen, K. Xu, Y. Tong, X. Li, S. Tao, Z. Fang, W. Chu, X. Wu, C. Wu, *Inorg. Chem. Front.* **2016**, *3*, 236–242.
- [27] B. Zhang, C. Xiao, S. Xie, J. Liang, X. Chen, Y. Tang, *Chem. Mater.* **2016**, *28*, 6934–6941.
- [28] M. Jiang, Y. Li, Z. Lu, X. Sun, X. Duan, *Inorg. Chem. Front.* **2016**, *3*, 630–634.
- [29] Z. Xing, Q. Li, D. Wang, X. Yang, X. Sun, *Electrochim. Acta* **2016**, *191*, 841–845.
- [30] L. Han, X. Y. Yu, X. W. Lou, *Adv. Mater.* **2016**, *28*, 4601–4605.

Manuscript received: February 16, 2017  
Revised manuscript received: March 16, 2017  
Accepted manuscript online: April 11, 2017  
Version of record online: June 13, 2017